Collective modes of a spin-orbit-coupled Bose-Einstein condensate: A hydrodynamic approach

Wei Zheng* and Zhibing Li

School of Physics and Engineering, Sun Yat-sen University, Guangzhou, People's Republic of China

(Received 4 February 2012; revised manuscript received 30 March 2012; published 9 May 2012)

We studied the collective modes of a Bose-Einstein condensate (BEC) with spin-orbit coupling. We developed the hydrodynamic equations for spin-orbit coupled BECs and used them to study collective modes in the plane-wave phase and large Rabi coupling regime for both a uniform BEC and a BEC in a harmonic trap. In the homogeneous situation, we obtained energy spectra of elementary excitations and found that the spin-orbit coupling can increase the effective mass of the atoms, which will suppress the sound velocity. The spin-orbit coupling can also change the spin mixing, which will modify the interaction energy, and may lead to an enhancement of sound velocity. The competition between these two effects gives the behavior of sound velocity. In a harmonic trap, we found that the dipole mode and the breathing mode are coupled together in the plane-wave phase, and these two modes have a $\pi/2$ phase difference, because the spin-orbit coupling and the interaction are not invariant under spin rotation. However, in the large Rabi coupling regime, the dipole mode and the breathing mode are decoupled due to the symmetry restriction.

DOI: 10.1103/PhysRevA.85.053607 PACS number(s): 03.75.Kk, 05.30.Jp, 67.85.De, 67.85.Fg

I. INTRODUCTION

Spin-orbit (SO) coupling is an interaction between a quantum particle's spin and its momentum. SO coupling plays an important role in condensed-matter physics. In electronic systems, it leads to some novel concepts, such as the quantum spin Hall effect and topological insulators [1], which have potential applications in spintronics and topological quantum computations. On the other hand, in cold-atom systems, a main subject is to simulate condensed-matter physics with dilute neutral atoms. Since atoms are neutral, they cannot interact with external electromagnetic fields. However, a synthetic gauge field, both Abelian or non-Abelian, can be coupled to neutral atoms by engineering the interactions between atoms and laser fields (for a review, see [2]). SO coupling is the simplest non-Abelian gauge potential, which is spatially independent. During 2009 to 2011, the NIST Group has successively realized uniform vector potentials [3], synthetic magnetic fields [4], electric fields [5], and SO coupling in a ^{87}Rb Bose-Einstein condensate (BEC) [6], which is a combination of equal Rashba and Dresselhaus strengths. The SO-coupled BECs began to attract attention over last few years. Their ground-state properties [7–9], fluctuations above the ground state [10,11], and SO-coupled BECs with other cold-atom techniques, such as dipole-dipole interactions, optical lattice and rotating trap [12], have been studied. Recently, SO-coupled degenerate Fermi gases have also been realized with ^{40}K atoms [13].

In cold-atom systems, collective modes, which are the low-energy excitations of a quantum gas, can be measured precisely [14,15]. Measuring the collective modes can help us to understand the physics of a quantum many-body system [16]. By measuring the splitting between two quadrupole modes, one can probe the angular momentum of a rotating BEC [17]. Studying scissors modes can give us direct evidence for superfluidity of a trapped BEC [18]. Observation of a damped dipole mode of a one-dimensional BEC in a combined harmonic trap and optical lattice demonstrates the important role of quantum fluctuations in an optical lattice [19]. Measurement of breathing modes allows us to test the Lee-Huang-Yang correction beyond the mean-field theory of a strongly interacting quantum gas [20]. Recently, the center-of-mass motion of BECs under artifical gauge potential has be studied by numerical computation [21] and by experiment [22,23].

There are various methods of studying the collective modes, such as the sum rule method, the hydrodynamic approach, and the variational method. The hydrodynamic approach describes a quantum liquid or gas using few variables, such as densities and velocities. For a BEC in a trap, hydrodynamic equations are valid in the Thomas-Fermi (TF) regime, $Na_s/a_{ho} \gg 1$, where the interaction energy dominates the dynamics of the condensate [16]. (Here N is the number of atoms, a_s is the s-wave scattering length, and a_{ho} is the length of the harmonic trap.)

In this paper, we studied the collective modes of a BEC with SO coupling realized in the NIST experiments. We developed the hydrodynamic equations for SO-coupled BECs, and used them to study the low-energy excitations in the plane-wave phase and large Rabi coupling regime both for a uniform BEC and a BEC in a trap. In the homogeneous situation, we obtained an energy spectrum of elementary excitations. In the long-wavelength limit, the elementary excitation is the sound wave in the condensate. We found that SO coupling can increase the single-particle effective mass of the atoms, which will suppress the sound velocity. However, SO coupling can also change the spin mixing, which will modify the interaction energy, and may lead to an enhancement of sound velocity. The competition between these two effects gives the behavior of sound velocity both in the plane-wave phase and in the large Rabi coupling regime. Then we studied the collective modes of a SO-coupled BEC in a harmonic trap. We found that in the plane-wave phase, the dipole mode and the breathing mode are coupled together, and they have a $\pi/2$ phase shift. However, in the large Rabi coupling regime, the dipole mode and the breathing

*zhengwei8796@gmail.com

mode are decoupled. We did not investigate the collective modes in the stripe phase because we cannot find an analytic or perturbation ground-state condensate wave function for the stripe phase which satisfies the Gross-Pitaevskii equations of a SO-coupled BEC.

II. THE MODEL AND HYDRODYNAMIC EQUATIONS

The effective Hamiltonian of SO-coupled Bosons in the NIST experiments is given by [6,8]:

$$H = \int d^3r \left(\hat{\Psi}^\dagger H_s \hat{\Psi} + \frac{1}{2} g_{11} \hat{n}_1^2 + \frac{1}{2} g_{22} \hat{n}_1^2 + g_{12} \hat{n}_1 \hat{n}_2 \right), \tag{1}$$

where $\hat{\Psi}^\dagger = (\hat{\psi}_1^\dagger, \hat{\psi}_2^\dagger)$ and $\hat{n}_j(\mathbf{r}) = \hat{\psi}_j^\dagger(\mathbf{r})\hat{\psi}_j(\mathbf{r})$, $j = 1,2$. $\hat{\psi}_{1,2}(\mathbf{r})$ are the field operators of two-component bosons (spin-up and spin-down). g_{ij} is the interaction strength between the atoms. H_s is the single-particle Hamiltonian, which is given by

$$H_s = \frac{1}{2m}(-i\partial_x - k_0\sigma_z)^2 - \frac{1}{2m}\partial_y^2 - \frac{1}{2m}\partial_z^2 + \Omega\sigma_x + h\sigma_z + V(r). \tag{2}$$

Here m is the mass of the atoms; Ω is the Rabi coupling between spin up and spin down. $k_0\sigma_z$ is the vector potential; h is the Zeeman splitting between spin up and spin down; and $V(r)$ is the trapping potential. Here we set $\hbar = 1$.

Consider a simple case with $h = 0$, $V(r) = 0$, $g_{11} = g_{22} = g$, and $g_{12} = \eta g$. One can see in this situation that the Hamiltonian is invariant under space inversion. When $\eta = 1$, the interactions between atoms are SU(2) invariant under spin rotation. However, in general, $\eta \neq 1$, and the SU(2) symmetry is broken. Since the SO coupling here is only in the x direction, we can treat the system as a one-dimensional system. The single-particle Hamiltonian is reduced into

$$H_s = \frac{1}{2m}(-i\partial_x - k_0\sigma_z)^2 + \Omega\sigma_x. \tag{3}$$

The single-particle spectrum can be obtained by diagonalizing (3):

$$\varepsilon_\pm(k) = \frac{1}{2m}\left(k^2 + k_0^2\right) \pm \sqrt{(k_0 k/m)^2 + \Omega^2}. \tag{4}$$

There are two branches of a single-particle spectrum. When $\Omega < k_0^2/m$, the lower branch has a double-well structure, with two degenerate single-particle ground states at $k = \pm k_m = \pm k_0\sqrt{1 - (\frac{\Omega}{k_0^2/m})^2}$ [see Fig. 2(a)]. When $\Omega > k_0^2/m$, the lower branch has only one minimum at $k = 0$ [see Fig. 6(a)]. The single-particle wave functions in the upper and lower branch are given by

$$\phi_k^{\mathrm{up}}(x) = \frac{1}{\sqrt{L}} \exp(ikx) \begin{pmatrix} \cos(\gamma_k/2) \\ \sin(\gamma_k/2) \end{pmatrix}, \tag{5}$$

$$\phi_k^{\mathrm{low}}(x) = \frac{1}{\sqrt{L}} \exp(ikx) \begin{pmatrix} -\sin(\gamma_k/2) \\ \cos(\gamma_k/2) \end{pmatrix}, \tag{6}$$

where L is the length of the system, and $\sin\gamma_k = \Omega/\sqrt{(k_0 k/m)^2 + \Omega^2}$. The single-particle wave function reveals that the direction of the spin is coupled to the momentum of the atom. When the momentum of an atom changes, the direction of its spin will rotate, and $\langle\sigma_z\rangle$ will also be changed. This is the essence of SO coupling.

In the $\Omega < k_0^2/m$ regime, assume that all atoms condense on a superposition state of the two degenerate single-particle states in the lower branch. The condensate wave function can be written as

$$\psi(x) = \sqrt{N}\left[\cos\frac{\chi}{2}\phi_{k_m}^{\mathrm{low}}(x) + \sin\frac{\chi}{2}\phi_{-k_m}^{\mathrm{low}}(x)\right], \tag{7}$$

where $\cos(\chi/2)$ and $\sin(\chi/2)$ are the superposition coefficients. Substituting Eq. (7) into the Hamiltonian (1), one obtains the mean-field energy up to a constant, which is a function of χ,

$$E = \tfrac{1}{4}Ng\rho\{[2 + (\eta - 1)\sin^2\gamma_{k_m}] + \tfrac{1}{2}\sin^2\chi(2\cos^2\gamma_{k_m} + \sin^2\gamma_{k_m})(\eta - \eta_c)\}, \tag{8}$$

where $\rho = N/L$ is the average density of the condensate, and η_c is given by

$$\eta_c = \frac{2 - \tan^2\gamma_{k_m}}{2 + \tan^2\gamma_{k_m}}. \tag{9}$$

Minimizing the mean-field energy with respect to χ, we find two distinct phases. For $\eta < \eta_c$, we have $\sin^2\chi = 1$. This is the so-called stripe phase, in which atoms condense on a superposition state of $k = k_m$ and $k = -k_m$. For $\eta > \eta_c$, we have $\sin^2\chi = 0$. This is the plane-wave phase, in which atoms condense on a single plane-wave state $k = k_m$ or $k = -k_m$. When increasing η across η_c, there will be a quantum phase transition from the stripe phase to the plane-wave phase [8]. The total density of this system can be obtained from a condensate wave function (7),

$$\rho(x) = \frac{N}{L}(1 + \sin\chi\sin\gamma_{k_m}\cos 2k_m x). \tag{10}$$

One can see that in the stripe phase, the total density is modulated by a wave vector $2k_m$, while in the plane-wave phase, the density is uniform. The stripe phase breaks the translational symmetry, while the plane wave breaks the time-reversal symmetry and parity symmetry. They both break the U(1) gauge symmetry of total phase.

In the $\Omega > k_0^2/m$ regime, most atoms condense at the $k = 0$ state. Therefore, the condensate wave function can be written as

$$\psi(x) = \sqrt{\frac{N}{L}} \begin{pmatrix} -1/\sqrt{2} \\ 1/\sqrt{2} \end{pmatrix}, \tag{11}$$

and the mean-field energy is

$$E = \tfrac{1}{4}Ng\rho(1 + \eta). \tag{12}$$

In the $\Omega > k_0^2/m$ regime, the condensate also breaks the U(1) gauge symmetry of the total phase. The phase diagram of this SO-coupled BEC is shown in Fig. 1. In this paper, we consider only the collective modes in the plane-wave phase and in the $\Omega > k_0^2/m$ regime.

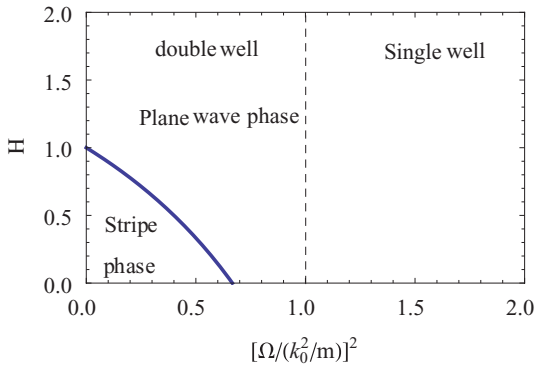

FIG. 1. (Color online) Phase diagram of a SO-coupled BEC. When $\Omega < k_0^2/m$, the lower branch of the single-particle spectrum has a double-well structure. When $\Omega > k_0^2/m$, the lower branch has only one minimum. The phase boundary of the stripe phase is determined by Eq. (9).

From Hamiltonian (1), the time-dependent Gross-Pitaevskii (GP) equations of SO-coupled BECs are given by

$$i\partial_t\psi_1 = \left[\frac{1}{2m}(-i\partial_x - k_0)^2 + V(x) + g|\psi_1|^2 + \eta g|\psi_2|^2 - \mu\right]\psi_1 + \Omega\psi_2, \tag{13}$$

$$i\partial_t\psi_2 = \left[\frac{1}{2m}(-i\partial_x + k_0)^2 + V(x) + g|\psi_2|^2 + \eta g|\psi_1|^2 - \mu\right]\psi_2 + \Omega\psi_1, \tag{14}$$

where μ is the chemical potential and ψ_j are the condensate wave functions of two components. Let $\psi_j = \sqrt{\rho_j}\exp(i\theta_j)$; the real parts of Eqs. (13) and (14) give

$$-\frac{\partial\theta_1}{\partial t} = -\frac{1}{2m}\frac{\partial_x^2\sqrt{\rho_1}}{\sqrt{\rho_1}} + \frac{1}{2m}(\partial_x\theta_1 - k_0)^2 + V(x) + g\rho_1 + \eta g\rho_2 - \mu + \Omega\sqrt{\frac{\rho_2}{\rho_1}}\cos(\theta_1 - \theta_2), \tag{15}$$

$$-\frac{\partial\theta_2}{\partial t} = -\frac{1}{2m}\frac{\partial_x^2\sqrt{\rho_2}}{\sqrt{\rho_2}} + \frac{1}{2m}(\partial_x\theta_2 + k_0)^2 + V(x) + g\rho_2 + \eta g\rho_1 - \mu + \Omega\sqrt{\frac{\rho_1}{\rho_2}}\cos(\theta_1 - \theta_2), \tag{16}$$

respectively, and the imaginary parts give

$$\frac{\partial\rho_1}{\partial t} = -\frac{1}{m}\partial_x\left[\rho_1(\partial_x\theta_1 - k_0)\right] - 2\Omega\sqrt{\rho_1\rho_2}\sin(\theta_1 - \theta_2), \tag{17}$$

$$\frac{\partial\rho_2}{\partial t} = -\frac{1}{m}\partial_x\left[\rho_2(\partial_x\theta_2 + k_0)\right] + 2\Omega\sqrt{\rho_1\rho_2}\sin(\theta_1 - \theta_2). \tag{18}$$

Those equations about ρ_j and θ_j are so-called hydrodynamic equations for SO-coupled BECs. The low-energy excitations can be obtained by considering small deviations from the ground state.

III. THE EXCITATIONS OF A HOMOGENEOUS BEC IN THE PLANE-WAVE PHASE

First let us consider the low-energy excitations for a homogeneous SO-coupled BEC in the plane-wave phase, where the external potential $V(r)$ is a constant. The first step is to find out the ground-state condensate wave function satisfying the GP equations. Since it is difficult to find an analytic ground-state wave function, we employed a perturbation treatment. Considering $\Omega \ll k_0^2/m$, the term $\Omega\sigma_x$ can be treated as a perturbation. One obtains the ground-state condensate wave function in the plane-wave phase up to second order of Ω as

$$\Psi = \sqrt{\rho}\exp(ik_0x)\begin{pmatrix}1 - \Omega^2/2f^2\\ -\Omega/f\end{pmatrix}, \tag{19}$$

where $f = 2k_0^2/m + (\eta - 1)g\rho$ and the corresponding chemical potential is $\mu = g\rho - \frac{2k_0^2/m}{f^2}\Omega^2$. It is easy to verify that the condensate wave function (19) satisfies the GP equations (13) and (14) up to Ω^2. This condensate wave function gives the densities and phases of spin-up and spin-down components in ground state as $\rho_1^g = \rho(1 - \Omega^2/f^2)$, $\rho_2^g = \rho\Omega^2/f^2$ and $\theta_1^g = k_0x$, $\theta_2^g = k_0x + \pi$. We note that the phase difference between spin-up and spin-down components is locked to π by Rabi coupling Ω in the ground state. We substitute $\rho_{1,2}^g$ and $\theta_{1,2}^g$ into the hydrodynamic equations (15)–(18), and find that they satisfy the hydrodynamic equations up to Ω^2. That implies $\rho_{1,2}^g$ and $\theta_{1,2}^g$ are the equilibrium solutions of the SO-coupled hydrodynamic equations.

Considering small fluctuations of densities and phases above the ground state $\rho_j = \rho_j^g + \delta\rho_j$, $\theta_j = \theta_j^g + \delta\theta_j$, substituting the fluctuations into the hydrodynamic equations, and keeping to linear terms, we obtain

$$\frac{\partial\delta\rho_1}{\partial t} = -\frac{\rho_1^g}{m}\partial_x^2\delta\theta_1 + 2\Omega\sqrt{\rho_1^g\rho_2^g}\,(\delta\theta_1 - \delta\theta_2), \tag{20}$$

$$\frac{\partial\delta\rho_2}{\partial t} = -\frac{\rho_2^g}{m}\partial_x^2\delta\theta_2 - 2\Omega\sqrt{\rho_1^g\rho_2^g}\,(\delta\theta_1 - \delta\theta_2) - \frac{2k_0}{m}\partial_x\delta\rho_2, \tag{21}$$

$$-\frac{\partial\delta\theta_1}{\partial t} = -\frac{1}{4m\rho_1^g}\partial_x^2\delta\rho_1 + g\delta\rho_1 + \eta g\delta\rho_2 - \frac{\Omega}{2}\left(\frac{1}{\sqrt{\rho_1^g\rho_2^g}}\delta\rho_2 - \sqrt{\frac{\rho_2^g}{\rho_1^{g3}}}\delta\rho_1\right), \tag{22}$$

$$-\frac{\partial\delta\theta_2}{\partial t} = -\frac{1}{4m\rho_2^g}\partial_x^2\delta\rho_2 + g\delta\rho_2 + \eta g\delta\rho_1 - \frac{\Omega}{2}\left(\frac{1}{\sqrt{\rho_1^g\rho_2^g}}\delta\rho_1 - \sqrt{\frac{\rho_1^g}{\rho_2^{g3}}}\delta\rho_2\right) + \frac{2k_0}{m}\partial_x\delta\theta_2. \tag{23}$$

These equations describe the fluctuations of a homogeneous SO-coupled BEC in the plane-wave phase. To find out traveling-wave solutions, we assume

$$\delta\rho_j(x,t) = \delta\rho_j\cos(kx - \omega t), \tag{24}$$

$$\delta\theta_j(x,t) = \delta\theta_j\sin(kx - \omega t). \tag{25}$$

Substituting these ansatzes into Eqs. (20)–(23), one obtains an eigenequation as

$$\begin{pmatrix} 0 & 0 & \frac{\rho_1^g k^2}{m} + 2\Omega\sqrt{\rho_1^g\rho_2^g} & -2\Omega\sqrt{\rho_1^g\rho_2^g} \\ 0 & \frac{2k_0k}{m} & -2\Omega\sqrt{\rho_1^g\rho_2^g} & \frac{\rho_2^g k^2}{m} + 2\Omega\sqrt{\rho_1^g\rho_2^g} \\ \frac{k^2}{4m\rho_1^g} + g + \frac{\Omega}{2}\sqrt{\frac{\rho_2^g}{\rho_1^{g3}}} & \eta g - \frac{\Omega}{2}/\sqrt{\rho_1^g\rho_2^g} & 0 & 0 \\ \eta g - \frac{\Omega}{2}/\sqrt{\rho_1^g\rho_2^g} & \frac{k^2}{4m\rho_2^g} + g + \frac{\Omega}{2}\sqrt{\frac{\rho_1^g}{\rho_2^{g3}}} & 0 & \frac{2k_0k}{m} \end{pmatrix} \begin{pmatrix} \delta\rho_1 \\ \delta\rho_2 \\ \delta\theta_1 \\ \delta\theta_2 \end{pmatrix} = \omega \begin{pmatrix} \delta\rho_1 \\ \delta\rho_2 \\ \delta\theta_1 \\ \delta\theta_2 \end{pmatrix}.$$

Numerically solving this eigenequation, one obtains the excitation spectrum of a SO-coupled BEC in the plane-wave phase, which is displayed in Fig. 2(b). The excitation spectrum has two branches, consisting of the single-particle spectrum. The lower branch is gapless, which is a Goldstone mode, corresponding to the spontaneous breaking of U(1) gauge symmetry of the total phase. The upper branch is gapped, since the Rabi coupling $\Omega\sigma_x$ locks the relative phase between spin-up and spin-down components, so the fluctuations of relative phase will cost finite energy.

We note that the spectrum of elementary excitation is unsymmetrical under $k \to -k$. In the plane-wave phase, most atoms condense in the $k = k_m$ or $k = -k_m$ state, so the parity symmetry is spontaneously broken. However, at long wavelength, $k \to 0$, the excitation spectrum is symmetric and linear, $\omega(k) = c\,|k|$, corresponding to the sound wave in the condensate, and c is just the sound velocity. By tuning the coupling Ω and interaction parameter η, one can change the sound velocity. The dependence of sound velocity c on Ω and η is displayed in Fig. 3, where $\Delta c = c - c_0$ and $c_0 = \sqrt{g\rho/m}$ is the sound velocity in a BEC without SO coupling. From Fig. 3(a), one can read that Δc is proportional to Ω^2. The proportionality coefficient is negative when $\eta < 3$ and positive when $\eta > 3$. At $\eta_0 = 3$, $\Delta c = 0$ and does not change with Ω.

One can employ a phenomenological analysis to explain this behavior. The sound velocity of a gas is defined as

$$c = \sqrt{\frac{K}{\rho m_S^*}}, \tag{26}$$

where $K = \rho^2\partial\mu/\partial\rho$ is the compressibility, and m_S^* is the effective mass of particles. In the plane-wave phase, most atoms condense at state $k = k_m$, so the chemical potential can be obtained up to Ω^2 from Eq. (8),

$$\mu = -\frac{k_0^2}{2m}\left(\frac{\Omega}{k_0^2/m}\right)^2 + \rho g\left[1 + \left(\frac{\Omega}{k_0^2/m}\right)^2\frac{(\eta-1)}{2}\right]. \tag{27}$$

This formula is consistent with $\mu = g\rho - \frac{2k_0^2/m}{f^2}\Omega^2$, obtained by solving SO-coupled GP equations, in the weakly interacting region, $g\rho \ll 2k_0^2/m$. The first term of Eq. (27) comes from lowering the zero energy point of a single-particle spectrum. It does not affect the excitation properties of condensates and can be removed. The second term reveals how Ω affects the interaction energy. In general, $\eta \neq 1$, which means the interactions between the spin-up and spin-down components are different with the one between the same spin components. So from Eq. (6), when one increases Ω, spin mixing will be increased, and that will change the interaction energy of condensates. From another aspect, atoms condense at $k = k_m$ in the plane-wave phase, so the effective mass m_S^* at k_m can be calculated from the single-particle spectrum:

$$\frac{1}{m_S^*(k_m)} = \left.\frac{\partial^2\varepsilon_-(k)}{\partial k^2}\right|_{k_m} = \frac{1}{m}\left[1 - \left(\frac{\Omega}{k_0^2/m}\right)^2\right]. \tag{28}$$

Substituting effective mass (28) and chemical potential (27) into (26), one obtains the sound velocity up to second order of Ω as

$$\frac{\Delta c}{c_0} \approx \frac{1}{4}\left(\frac{\Omega}{k_0^2/m}\right)^2(\eta - 3). \tag{29}$$

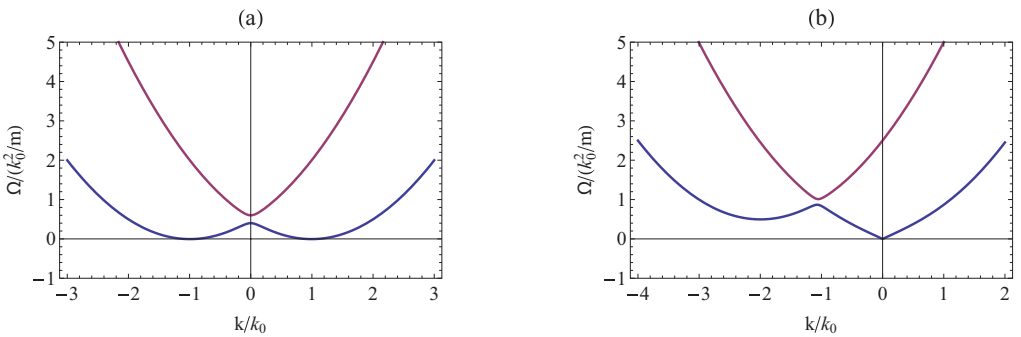

FIG. 2. (Color online) (a) Single-particle spectrum of an atom with NIST-stype SO coupling at regime $\Omega < k_0^2/m$. (b) Elementary excitation spectrum of a SO-coupled BEC in the plane-wave phase. Here $\Omega/(k_0^2/m) = 0.1$, $g\rho/(k_0^2/m) = 0.5$, and $\eta = 2$.

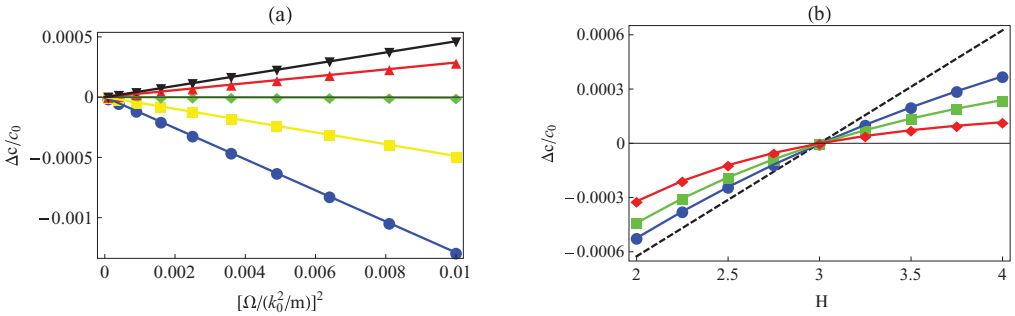

FIG. 3. (Color online) (a) Sound velocity of a SO-coupled BEC depending on $\Omega/(k_0^2/m)$ in the plane-wave phase. Here $\Delta c = c - c_0$, $g\rho/(k_0^2/m) = 0.5$, and $\eta = 2, 2.5, 3, 3.5, 4$ for circular, square, diamond, triangular, and inverted triangle points, respectively. (b) Sound velocity of a SO-coupled BEC depending on η in the plane-wave phase. Here $\Omega/(k_0^2/m) = 0.05$ and $g\rho/(k_0^2/m) = 1/8, 1/4, 1/2$ for circular, square, and diamond points, respectively. The dashed line represents the results from Eq. (29).

We note that at $\eta_0 = 3$, $c = c_0$, which is consistent with the results from solving hydrodynamic equations. The changes of sound velocity by tuning Ω come from two effects. One is the change of single-particle spectrum, which modifies the effective mass. The other is the change of interaction energy, which leads to the changing of chemical potential. The behavior of sound velocity is due to the competition between these two effects.

IV. COLLECTIVE MODES OF THE PLANE-WAVE PHASE IN A HARMONIC TRAP

Since most experiments of cold atoms are carried out in a harmonic trap, it is natural to investigate the collective modes of a SO-coupled BEC in a trap. To study the collective modes in a harmonic trap, we first employ the local density approximation (LDA), assuming the trapping potentials are weak compared to the interaction energy of a BEC. One obtains the TF ground-state condensate wave function in the trap up to second-order perturbation as

$$\Psi = \sqrt{\rho(x)}\exp(ik_0x)\begin{pmatrix}1-\Omega^2/2f^2(x)\\ -\Omega/f(x)\end{pmatrix}, \tag{30}$$

where the local total density $\rho^g(x) = \frac{\mu - V(x)}{g}$, and $f(x) = 2k_0^2/m + (\eta-1)g\rho(x)$. Based on this ground state, the equations of fluctuations in the trap become

$$\frac{\partial\delta\rho_1}{\partial t} = -\frac{\rho_1^g}{m}\partial_x^2\delta\theta_1 - \partial_x\rho_1^g\partial_x\delta\theta_1 + 2\Omega\sqrt{\rho_1^g\rho_2^g}\,(\delta\theta_1 - \delta\theta_2), \tag{31}$$

$$\frac{\partial\delta\rho_2}{\partial t} = -\frac{\rho_2^g}{m}\partial_x^2\delta\theta_2 - \partial_x\rho_2^g\partial_x\delta\theta_2 - 2\Omega\sqrt{\rho_1^g\rho_2^g}\,(\delta\theta_1 - \delta\theta_2) - \frac{2k_0}{m}\partial_x\delta\rho_2, \tag{32}$$

$$-\frac{\partial\delta\theta_1}{\partial t} = g\delta\rho_1 + \eta g\delta\rho_2 - \frac{\Omega}{2}\left(\frac{1}{\sqrt{\rho_1^g\rho_2^g}}\delta\rho_2 - \sqrt{\frac{\rho_2^g}{\rho_1^{g3}}}\delta\rho_1\right), \tag{33}$$

$$-\frac{\partial\delta\theta_2}{\partial t} = g\delta\rho_2 + \eta g\delta\rho_1 - \frac{\Omega}{2}\left(\frac{1}{\sqrt{\rho_1^g\rho_2^g}}\delta\rho_1 - \sqrt{\frac{\rho_1^g}{\rho_2^{g3}}}\delta\rho_2\right) + \frac{2k_0}{m}\partial_x\delta\theta_2, \tag{34}$$

where we have ignored the so-called "quantum pressure terms" [24]. To solve those equations and obtain the collective modes, we assume that the fluctuations are as follows:

$$\delta\rho_1 = X_1(x)\cos\omega t + Y_1(x)\sin\omega t, \tag{35}$$

$$\delta\rho_2 = X_1(x)\cos\omega t + Y_1(x)\sin\omega t, \tag{36}$$

$$\delta\theta_1 = \alpha_1(x)\cos\omega t + \beta_1(x)\sin\omega t, \tag{37}$$

$$\delta\theta_2 = \alpha_1(x)\cos\omega t + \beta_1(x)\sin\omega t. \tag{38}$$

Substituting Eqs. (35)–(38) into Eqs. (31)–(34), one obtains

$$\omega X_1 = -\frac{\rho_1^g}{m}\partial_x^2\beta_1 - \frac{1}{m}\partial_x\rho_1^g\partial_x\beta_1 + 2\Omega\sqrt{\rho_1^g\rho_2^g}\,(\beta_1 - \beta_2), \tag{39}$$

$$\omega Y_1 = \frac{\rho_1^g}{m}\partial_x^2\delta\alpha_1 + \frac{1}{m}\partial_x\rho_1^g\partial_x\alpha_1 - 2\Omega\sqrt{\rho_1^g\rho_2^g}\,(\alpha_1 - \alpha_2), \tag{40}$$

$$\omega X_2 = -\frac{\rho_2^g}{m}\partial_x^2\beta_2 - \frac{1}{m}\partial_x\rho_2^g\partial\beta_2 - 2\Omega\sqrt{\rho_1^g\rho_2^g}\,(\beta_1 - \beta_2) - \frac{2k_0}{m}\partial_x Y_2, \tag{41}$$

$$\omega Y_2 = \frac{\rho_2^g}{m}\partial_x^2\alpha_2 + \frac{1}{m}\partial_x\rho_2^g\partial_x\alpha_2 + 2\Omega\sqrt{\rho_1^g\rho_2^g}\,(\alpha_1 - \alpha_2) + \frac{2k_0}{m}\partial_x X_2, \tag{42}$$

$$\omega\alpha_1 = -gY_1 - \eta gY_2 + \frac{\Omega}{2}\left(\frac{1}{\sqrt{\rho_1^g\rho_2^g}}Y_2 - \sqrt{\frac{\rho_2^g}{\rho_1^{g3}}}Y_1\right), \tag{43}$$

$$\omega\beta_1 = gX_1 + \eta gX_2 - \frac{\Omega}{2}\left(\frac{1}{\sqrt{\rho_1^g\rho_2^g}}X_2 - \sqrt{\frac{\rho_2^g}{\rho_1^{g3}}}X_1\right), \tag{44}$$

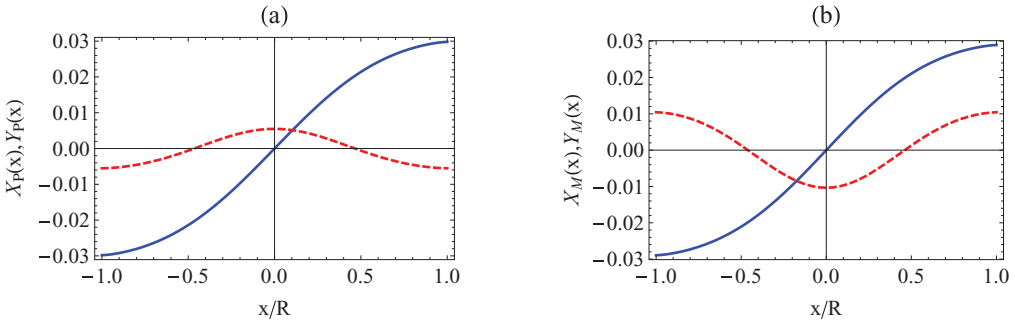

FIG. 4. (Color online) Profiles of collective modes of a SO-coupled BEC in a harmonic trap in the plane-wave phase. (a) The profile of total density. The solid line is $X_\rho(x)$, which is a dipole mode; the dashed line is $Y_\rho(x)$, which is a breathing mode. (b) The profile of spin polarization. The solid line is $X_M(x)$ and the dashed line is $Y_M(x)$. Here $\Omega/(k_0^2/m) = 0.25$, $\mu/\omega_0 = 45$, $\eta = 1.2$, and $(k_0^2/m)/\omega_0 = 4$.

$$\omega\alpha_2 = -gY_2 - \eta gY_1 + \frac{\Omega}{2}\left(\frac{1}{\sqrt{\rho_1^g\rho_2^g}}Y_1 - \sqrt{\frac{\rho_1^g}{\rho_2^{g3}}}Y_2\right) - \frac{2k_0}{m}\partial_x\beta_2, \tag{45}$$

$$\omega\beta_2 = gX_2 + \eta gX_1 - \frac{\Omega}{2}\left(\frac{1}{\sqrt{\rho_1^g\rho_2^g}}X_1 - \sqrt{\frac{\rho_1^g}{\rho_2^{g3}}}X_2\right) + \frac{2k_0}{m}\partial_x\alpha_2. \tag{46}$$

Numerically solving those equations, we obtain the frequencies of collective modes. Denoting total density fluctuation as $\delta\rho(x,t) = \delta\rho_1(x,t) + \delta\rho_2(x,t)$ and spin polarization fluctuation as $\delta M(x,t) = \delta\rho_1(x,t) - \delta\rho_2(x,t)$, we have

$$\delta\rho(x,t) = X_\rho(x)\cos(\omega t) + Y_\rho(x)\sin(\omega t), \tag{47}$$

$$\delta M(x,t) = X_M(x)\cos(\omega t) + Y_M(x)\sin(\omega t), \tag{48}$$

where $X_\rho(x) = X_1(x) + X_2(x)$, $X_M(x) = X_1(x) - X_2(x)$, $Y_\rho(x) = Y_1(x) + Y_2(x)$, and $Y_M(x) = Y_1(x) - Y_2(x)$. Here we focus on the lowest collective mode. Th profiles of the lowest collective mode are plotted in Fig. 4. It shows that $X_\rho(x)$ is a dipole mode, which is a center-of-mass oscillation of the condensate. (It is not an exact dipole mode as $X_\rho(x) \sim x$. It is a combination of dipole mode and other modes with odd parity, but the dipole mode gives the primary contributions.) $Y_\rho(x)$ is a breathing mode, which describes the oscillation of the size of the condensate. [It is not an exact breathing mode, $Y_\rho(x) \sim P_2(x)$, but a combination of other modes with even parity, but the breathing mode gives the primary contributions. Here $P_n(x)$ is the Legendre polynomial.] For a single-component BEC without SO coupling, the dipole mode and the breathing mode are decoupled and have different oscillation frequencies. However, in a SO-coupled BEC the dipole mode and the breathing mode are coupled together. In addition, from Eqs. (35)–(38), one can see that there is a $\pi/2$ phase difference between these two modes. When the center-of-mass of a SO-coupled BEC oscillates in the trap, the size of the BEC will also oscillate. $X_M(x)$ and $Y_M(x)$ show spatial distribution of spin polarization fluctuations, which can also be regarded as a Rabi oscillation.

When a particle oscillates in real space, due to the SO coupling, its spin will also oscillate. Since the interactions between the atoms are not invariant under SU(2) spin rotation in general, $\eta \neq 1$, oscillation of spin polarization in a condensate will induce an oscillation of interaction energy. As we know, in the harmonic trap the TF radius R of the condensate is determined by the balance of interaction energy and trapping potential. When the interaction energy changes, the size of the condensate will also change. Hence, the dipole oscillation in this system will induce the size oscillation of the condensate, which is just the breathing mode. From the discussion above, we note that the breathing mode has the same phase with the spin oscillations, whose phase is consistent with the oscillations of momentum. In addition, in the harmonic trap, the phase difference between momentum oscillation and center-of-mass oscillation, that is, the dipole mode, is just $\pi/2$. That explains why the dipole mode and the breathing mode have the $\pi/2$ phase difference. The coupling of the dipole mode and the breathing mode is a joint effect of SO coupling and SU(2) symmetry breaking of the spin invariance of interactions.

The oscillation frequencies, $\Delta\omega = \omega - \omega_0$, depending on Ω and η, are displayed in Fig. 5, where ω_0 is the trapping frequency. One can see that such a dependence is very similar to the one of sound velocities in a homogeneous SO-coupled BEC. That is because the dipole mode and the breathing mode of a trapped BEC can be regarded as the phonon modes with wave length $2R$ and R, respectively. However the transition point η_0, at which $\Delta\omega = 0$, is not a constant, but decreases with chemical potential [see Fig. 5(b)]. One can employ a semiclassical analysis to understand this phenomenon. Assume all the atoms condense in the single-particle state k in the lower branch during the dipole oscillation. Therefore, the kinetic energy and the interacting energy are the functions of k

$$E_K(k) = N\left[\frac{1}{2m}\left(k^2 + k_0^2\right) - \sqrt{(k_0k/m)^2 + \Omega^2}\right], \tag{49}$$

$$E_I(k) = \frac{1}{2}Ng\rho\left[1 + \frac{1}{2}(\eta - 1)\frac{\Omega^2}{(k_0k/m)^2 + \Omega^2}\right]. \tag{50}$$

We can expand them around equilibrium state $k = k_m$ to second order:

$$E_K(k)/N \approx \frac{1}{2m_S^*(k_m)}(k - k_m)^2, \tag{51}$$

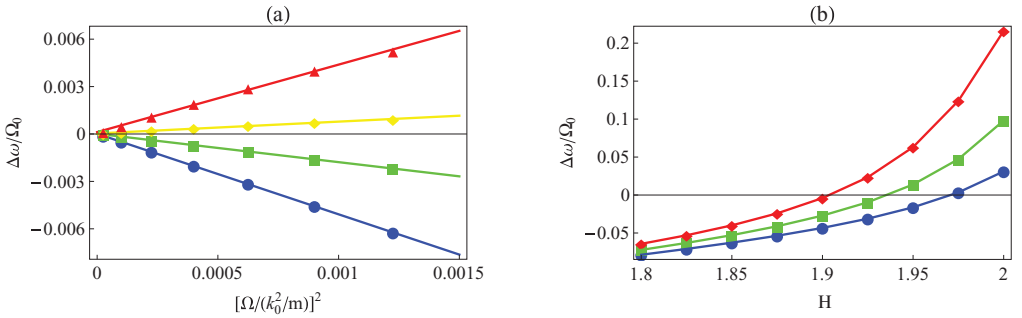

FIG. 5. (Color online) (a) Collective mode frequencies of a SO-coupled BEC in a harmonic trap versus $\Omega/(k_0^2/m)$ in the plane-wave phase. Here $\Delta\omega = \omega - \omega_0$ with ω_0 the trapping frequency. The circles, squares, diamonds, and triangles are for $\eta = 1.2$, 1.26, 1.3, and 1.32, respectively. We have used $\mu/\omega_0 = 50$ and $(k_0^2/m)/\omega_0 = 4$. (b) Frequencies depending on η in the plane-wave phase. Here $\Omega/(k_0^2/m) = 0.0125$ and $(k_0^2/m)/\omega_0 = 16$. The circles, squares, and diamonds are for $\mu/\omega_0 = 18$, 19, and 20, respectively.

$$E_{\mathrm{I}}(k)/N \approx \frac{1}{2m_{\mathrm{I}}^*(k_m)}(k-k_m)^2. \tag{52}$$

Here m_{S}^* is the effective mass coming from single particle spectrum (28), and m_{I}^* is the effective mass origin from the interaction between the particles:

$$\frac{1}{m_{\mathrm{I}}^*(k_m)} = \left.\frac{\partial E_{\mathrm{I}}(k)/N}{\partial k}\right|_{k_m} = \frac{1}{m}\left[\frac{3}{2}\left(\frac{\Omega}{k_0^2/m}\right)^2 \frac{g\rho\,(\eta-1)}{k_0^2/m}\right]. \tag{53}$$

Therefore, the total energy is

$$E/N = \frac{1}{2m^*}(k-k_m)^2 + \frac{1}{2}m\omega_0^2 x^2, \tag{54}$$

where $1/m^* = 1/m_{\mathrm{S}}^*(k_m) + 1/m_{\mathrm{I}}^*(k_m)$ is the total effective mass. From Eqs. (54) and (27), one can find the frequency shift of the dipole mode as

$$\frac{\Delta\omega}{\omega_0} \approx \frac{1}{2}\left(\frac{\Omega}{k_0^2/m}\right)^2\left[\frac{3}{2}\frac{\mu\,(\eta-1)}{k_0^2/m} - 1\right] \tag{55}$$

and obtains $\eta_0 \approx 1 + \frac{2}{3}\frac{k_0^2/m}{\mu}$. That explains the phenomenon that the η_0 decreases with the chemical potential shown in Fig. 5 qualitatively. When Ω increases, m_{S}^* increases, while m_{I}^* decreases. Similar to the behavior of the sound velocity in a homogeneous situation, the behavior of dipole mode frequency in harmonic trap is also the result of competition between the changes of a single-particle spectrum and interaction energy with Ω. However, the frequency shift given by Eq. (55) is not quantitatively consistent with the one obtained by the hydrodynamic approach because the assumption that all atoms are in the same single-particle state during the oscillation is not accurate.

V. LARGE RABI COUPLING REGIME

In the $\Omega > k_0^2/m$ regime, the lower branch of the single-particle spectrum becomes a single-well structure, and most atoms condense in the $k = 0$ state. One can find the ground-state condensate wave function as

$$\psi = \sqrt{\frac{\rho}{2}}\begin{pmatrix}-1\\1\end{pmatrix}, \tag{56}$$

which satisfies the GP equations of a SO-coupled BEC (13) and (14). The corresponding chemical potential is $\mu = k_0^2/2m - \Omega + g\rho(\eta+1)/2$. Considering the small fluctuations above the ground state, one find the equations of fluctuations in a uniform potential as

$$\frac{\partial\delta\rho_1}{\partial t} = -\frac{\rho}{2m}\partial_x^2\delta\theta_1 + \Omega\rho\,(\delta\theta_1 - \delta\theta_2) + \frac{k_0}{m}\partial_x\delta\rho_1, \tag{57}$$

$$\frac{\partial\delta\rho_2}{\partial t} = -\frac{\rho}{2m}\partial_x^2\delta\theta_2 - \Omega\rho\,(\delta\theta_1 - \delta\theta_2) - \frac{k_0}{m}\partial_x\delta\rho_2, \tag{58}$$

$$-\frac{\partial\delta\theta_1}{\partial t} = -\frac{1}{2m\rho}\partial_x^2\delta\rho_1 + g\delta\rho_1 + \eta g\delta\rho_2 - \frac{\Omega}{\rho}(\delta\rho_2 - \delta\rho_1) - \frac{k_0}{m}\partial_x\delta\theta_2, \tag{59}$$

$$-\frac{\partial\delta\theta_2}{\partial t} = -\frac{1}{2m\rho}\partial_x^2\delta\rho_2 + g\delta\rho_2 + \eta g\delta\rho_1 - \frac{\Omega}{\rho}(\delta\rho_1 - \delta\rho_2) + \frac{k_0}{m}\partial_x\delta\theta_2. \tag{60}$$

Solving those equations, one obtains the dispersion relation for the $\Omega > k_0^2/m$ case, which is plotted in Fig. 6(b). One can see the dispersion relation has also two branches. The dispersion relation is symmetric under $k \to -k$, because the ground state in $\Omega > k_0^2/m$ regime is invariant under space inversion. Just as the previous analysis, the effective mass m_{S}^* at $k = 0$ is $m_{\mathrm{S}}^{*-1}(0) = m^{-1}(1 - \frac{k_0^2/m}{\Omega})$ and compressibility $K = \frac{1}{2}g\rho(1+\eta)$. One can find out the sound velocity as

$$\frac{c}{c_0} = \sqrt{\frac{1+\eta}{2}\left(1 - \frac{k_0^2/m}{\Omega}\right)}. \tag{61}$$

This formula fits well with the results calculated from hydrodynamic equations, shown in Fig. 7(a). Unlike the plane-wave phase, Ω only changes the effective mass $m_{\mathrm{S}}^{*-1}(0)$, but does not change the compressibility. Because from Eq. (6), we know that at the $k = 0$ state, spin-up and spin-down components have equal populations, and spin polarization will not change with Ω. In the limit $\Omega \gg k_0^2/m$, $m_{\mathrm{S}}^*(0) \approx m$, the sound velocity is only dependent on η.

In a harmonic trap, employing LDA, one obtains the condensate wave function as

$$\psi = \sqrt{\frac{\rho^{\mathrm{g}}(x)}{2}}\begin{pmatrix}-1\\1\end{pmatrix}, \tag{62}$$

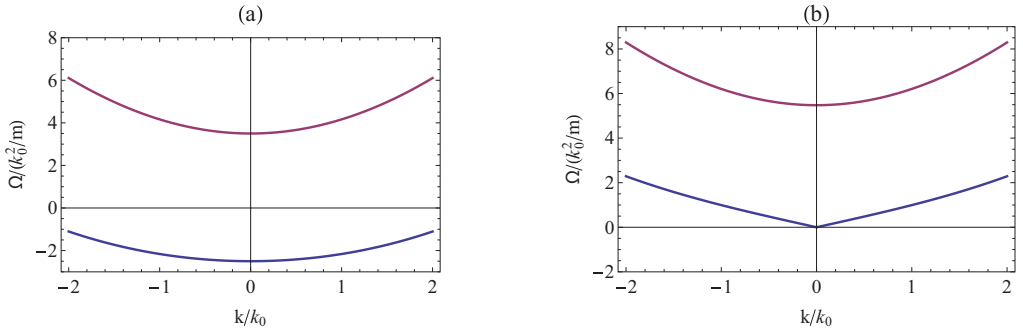

FIG. 6. (Color online) (a) Single-particle spectrum of an atom with NIST-type SO coupling in the $\Omega > k_0^2/m$ regime. (b) Elementary excitation spectrum of a SO-coupled BEC in the $\Omega > k_0^2/m$ regime. Here $\Omega/(k_0^2/m) = 3$, $g\rho/(k_0^2/m) = 1$, and $\eta = 2$.

where $\rho^g(x) = \frac{\mu - V(x)}{g(1+\eta)/2}$. So the fluctuation equations in the trap can be written as

$$\frac{\partial \delta\rho_1}{\partial t} = -\frac{\rho^g}{2m}\partial_x^2\delta\theta_1 - \frac{1}{2m}\partial_x\rho^g\partial_x\delta\theta_1 + \Omega\rho^g(\delta\theta_1 - \delta\theta_2) + \frac{k_0}{m}\partial_x\delta\rho_1, \tag{63}$$

$$\frac{\partial \delta\rho_2}{\partial t} = -\frac{\rho^g}{2m}\partial_x^2\delta\theta_2 - \frac{1}{2m}\partial_x\rho^g\partial_x\delta\theta_2 - \Omega\rho^g(\delta\theta_1 - \delta\theta_2) - \frac{k_0}{m}\partial_x\delta\rho_2, \tag{64}$$

$$-\frac{\partial \delta\theta_1}{\partial t} = g\delta\rho_1 + \eta g\delta\rho_2 - \frac{\Omega}{\rho^g}(\delta\rho_2 - \delta\rho_1) - \frac{k_0}{m}\partial_x\delta\theta_2, \tag{65}$$

$$-\frac{\partial \delta\theta_2}{\partial t} = g\delta\rho_2 + \eta g\delta\rho_1 - \frac{\Omega}{\rho^g}(\delta\rho_1 - \delta\rho_2) + \frac{k_0}{m}\partial_x\delta\theta_2. \tag{66}$$

Just as in the plane-wave phase, we assume the fluctuations of densities and phases have the forms as (35)–(38). One obtains

$$\omega X_1 = -\left(-\frac{\rho^g}{2m}\partial_x^2 - \frac{1}{2m}\partial_x\rho^g\partial_x + \Omega\rho^g\right)\beta_1 + \Omega\rho^g\beta_2 - \frac{k_0}{m}\partial_x Y_1, \tag{67}$$

$$\omega Y_1 = \left(-\frac{\rho^g}{2m}\partial_x^2 - \frac{1}{2m}\partial_x\rho^g\partial_x + \Omega\rho^g\right)\alpha_1 - \Omega\rho^g\alpha_2 + \frac{k_0}{m}\partial_x X_1, \tag{68}$$

$$\omega X_2 = -\left(-\frac{\rho^g}{2m}\partial_x^2 - \frac{1}{2m}\partial_x\rho^g\partial_x + \Omega\rho^g\right)\beta_2 + \Omega\rho^g\beta_1 + \frac{k_0}{m}\partial_x Y_2, \tag{69}$$

$$\omega Y_1 = \left(-\frac{\rho^g}{2m}\partial_x^2 - \frac{1}{2m}\partial_x\rho^g\partial_x + \Omega\rho^g\right)\alpha_2 - \Omega\rho^g\alpha_1 - \frac{k_0}{m}\partial_x X_2, \tag{70}$$

$$\omega\alpha_1 = \left(g + \frac{\Omega}{\rho^g}\right)Y_1 + \left(\eta g - \frac{\Omega}{\rho^g}\right)Y_2 - \frac{k_0}{m}\partial_x\beta_1, \tag{71}$$

$$\omega\beta_1 = -\left(g + \frac{\Omega}{\rho^g}\right)X_1 - \left(\eta g - \frac{\Omega}{\rho^g}\right)X_2 + \frac{k_0}{m}\partial_x\alpha_1, \tag{72}$$

$$\omega\alpha_2 = \left(g + \frac{\Omega}{\rho^g}\right)Y_2 + \left(\eta g - \frac{\Omega}{\rho^g}\right)Y_1 + \frac{k_0}{m}\partial_x\beta_2, \tag{73}$$

$$\omega\beta_2 = -\left(g + \frac{\Omega}{\rho^g}\right)X_2 - \left(\eta g - \frac{\Omega}{\rho^g}\right)X_1 - \frac{k_0}{m}\partial_x\alpha_2. \tag{74}$$

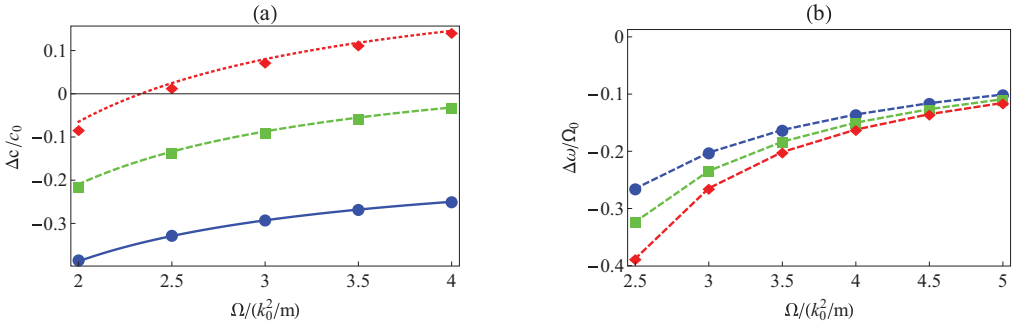

FIG. 7. (Color online) (a) Sound velocity of a SO-coupled BEC depending on $\Omega/(k_0^2/m)$ at regime $\Omega > k_0^2/m$. Here $\Delta c = c - c_0$, $g\rho/(k_0^2/m) = 0.1$, and $\eta = 0.5$, 1.5, 2.5, for circular, square, and diamond points, respectively. The solid, dashed, and dotted lines are corresponding results from Eq. (61). (b) Frequencies of the lowest mode (dipole mode) of a SO-coupled BEC in a harmonic trap versus $\Omega/(k_0^2/m)$ at regime $\Omega > k_0^2/m$. Here $\Delta\omega = \omega - \omega_0$ with ω_0 the trapping frequency. The circles, squares, and diamonds are for $\eta = 1.5$, 2, 2.5, respectively. We have used $\mu/\omega_0 = 10$ and $(k_0^2/m)/\omega_0 = 4$.

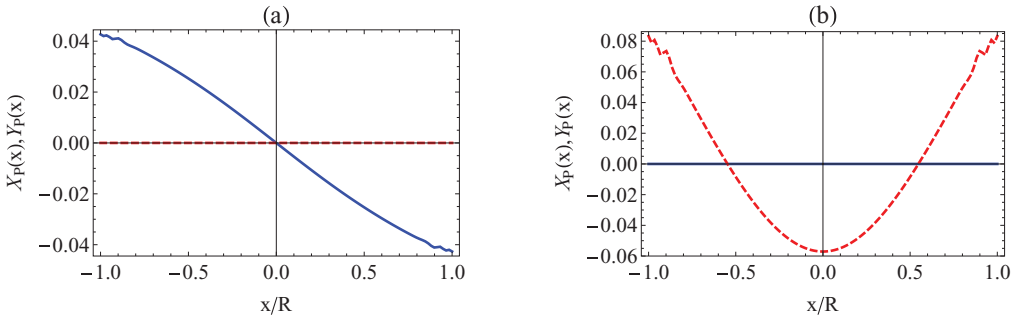

FIG. 8. (Color online) Profiles of collective modes of a SO-coupled BEC in a harmonic trap at $\Omega > k_0^2/m$ regime. (a) The profile of the lowest collective mode. The solid line is $X_\rho(x)$, which is a dipole mode; the dashed line is $Y_\rho(x)$. (b) The profile of the second-lowest collective mode. The solid line is $X_\rho(x)$ and the dashed line is $Y_\rho(x)$, which is a breathing mode. Here $\Omega/(k_0^2/m) = 2.5$, $\mu/\omega_0 = 10$, $\eta = 2$, and $k_0^2/\omega_0 = 4$.

Numerically solving these equations, one obtains the lowest collective mode and the second-lowest mode in a harmonic trap, which is plotted in Figs. 8(a) and 8(b), respectively. In the lowest mode, there is only dipole mode, $X_\rho \sim x, Y_\rho = 0$. In the second-lowest mode, there is only breathing mode, $X_\rho = 0$, $Y_\rho \sim P_2(x)$. That implies the dipole mode and the breathing mode are decoupled. From Eqs. (67)–(74), one can obtain

$$\omega X_\rho = -\left(-\frac{\rho^g}{2m}\partial_x^2 - \frac{1}{2m}\partial_x\rho^g\partial_x + \Omega\rho\right)\beta_\rho + \Omega\rho^g\beta_\rho - \frac{k_0}{m}\partial_x Y_M, \tag{75}$$

$$\omega Y_M = \left(-\frac{\rho^g}{2m}\partial_x^2 - \frac{1}{2m}\partial_x\rho^g\partial_x + \Omega\rho\right)\alpha_M + \Omega\rho^g\alpha_M + \frac{k_0}{m}\partial_x X_\rho, \tag{76}$$

$$\omega\alpha_M = \left(g - \eta g + \frac{2\Omega}{\rho^g}\right)Y_M - \frac{k_0}{m}\partial_x\beta_\rho, \tag{77}$$

$$\omega\beta_\rho = -(g + \eta g)X_\rho + \frac{k_0}{m}\partial_x\alpha_M, \tag{78}$$

where $\beta_\rho = \beta_1 + \beta_2$, $\alpha_M = \alpha_1 - \alpha_2$. One can see these equations are closed. X_ρ is decoupled with Y_ρ and coupled only with Y_M. One can understand this phenomenon by considering the interaction energy during the oscillation, $E_I(k)$ [see Eq. (50)]. In the plane-wave phase, we find $E_I(k)$ is unsymmetric about the equilibrium state $k = k_m$. Assume that during the dipole oscillation, the amplitude of the momentum oscillation is Δk. At $k_m - \Delta k$, the interaction energy of the condensate reaches it largest value, and so does the condensate size. At $k_m + \Delta k$ the interaction energy and the size of the condensate are smallest during the oscillation. So the period of the breathing mode matches with the dipole mode, and they can be coupled together. However, at regime $\Omega > k_0^2/2m$, $E_I(k)$ is symmetric about the equilibrium state at $k = 0$; the size of the condensate reaches its maximum at $k = 0$ and reaches its minimum at Δk and $-\Delta k$ during oscillation. If the breathing mode is coupled with dipole oscillation, the period of the center-of-mass oscillation will be twice that of size oscillation. They cannot be matched. So the mode which is dipole mode coupled with breathing mode cannot be an eigenmode of the condensate. The frequency shift of the dipole mode is plotted in Fig. 7(b). The dipole mode is not coupled with the breathing mode, so we cannot use the effective mass m_I^* from interaction energy to estimate the frequency shift. However, the dipole mode is coupled with other modes with odd parity. So the frequency shift is also dependent on η. From another point of view, the ground state at the $\Omega > k_0^2/2m$ regime is invariant under space inversion, so the collective modes above this ground state have certain parities. Coupling between the dipole mode and the breathing mode is forbidden.

VI. SUMMARY

We investigated the collective modes of a SO-coupled BEC in the plane-wave phase and in the large Rabi coupling regime, both for a homogeneous situation and in a harmonic trap, by solving the hydrodynamic equations. We developed the hydrodynamic equations for a SO-coupled BEC, which has been realized in the NIST experiments. Then we considered the small fluctuations above the ground state and found the equations for the fluctuations. By solving these equations, we obtained the low-energy excitations. In the homogeneous situation, the energy spectrum of elementary excitations was obtained. There are two branches in the elementary excitation spectrum: one has a gap, and other is gapless. The latter is the Goldstone mode. In the plane-wave phase the excitation spectrums is not symmetric under $k \to -k$, because the space-inversion symmetry is spontaneously breaking in the ground state. At long wavelength, the gapless mode is the sound wave in the condensate and has the linear dispersion $\omega(k) = c\,|k|$. We found that the sound velocity, c, can be tuned by changing the strength of the Rabi coupling Ω. When $\eta < 3$, increasing Ω will decrease the sound velocity; while $\eta > 3$, increasing Ω will lead to the increase of sound velocity. The SO coupling has two effects here. First, it changes the single-particle spectrum of atoms, so that increasing Ω will increase the effective mass m_S^* of the atoms. That will suppress the sound velocity. Second, SO coupling mixes spin-up and spin-down components, leading to the change of interaction energy. When $\eta > 1$, increasing Ω will enlarge the interaction energy and increase the compressibility of the condensate, leading to an increasing of sound velocity. These two effects have opposite influences on sound velocity

when $\eta > 1$. In the regime $\eta < 3$, the effective mass effect dominates the behavior of sound velocity, while in the regime of $\eta > 3$, the interaction energy effect plays the primary role. In the NIST experiment which used the hyperfine levels of ^{87}Rb, such large η is difficult to achieve. However, some proposals of artificial gauge potentials [2], involving the excited states of alkaline-earth-metal atoms, may provide large-enough η. On other hand, in the NIST experiment a magnetic field was applied to split the hyperfine states so that the Feshbach resonance is limited. For the proposals using the dark states without magnetic field [25,26], which may be achieved in further experiments, one can use the Feshbach resonance to tune the spin-dependent scattering length to achieve large η. In the $\Omega > k_0^2/m$ regime, the excitation spectrum is symmetric under $k \to -k$, because the ground state is invariant under space inversion. The changing of Ω will only change the effective mass, and not affect the interaction energy in $\Omega > k_0^2/m$ regime. In a trapped BEC, the sound can propagate when the phonon wave length is much smaller than the size of the system but larger than the healing length. The sound velocities can be measured [27]. The excitation spectrum can be also measured by Bragg scattering [28]. We expect an experiment to measure the sound velocities of the SO-coupled BEC.

In the harmonic trap, we find the dipole mode and the breathing mode are coupled together in the plane-wave phase. There is a $\pi/2$ phase difference between these two modes. Such coupling is the joint effect of SO coupling and broken invariance of SU(2) spin rotation. A small shift of the trap will excite both the center-of-mass motion and the oscillation of the condensate size. We emphasize that in the middle Ω regime, $\Omega \lesssim k_0^2/m$, the barrier between the double wells in the single-particle spectrum becomes very low, and the condensate will have a chance to tunnel into another well in momentum space during the dipole oscillation. Recently this tunneling phenomenon in momentum space has been observed in experiments [22]. Our hydrodynamic equations cannot describe this phenomenon. So we only consider the situation with small Ω and small oscillation amplitude so that the tunneling probability can be neglected. Because the dipole mode and the breathing mode can be regarded as sound waves in the trap with wavelengths $2R$ and R, the behavior of the oscillation frequency is similar to the one of sound velocity in the uniform condensate. When $\eta < \eta_0$, the effective mass m_S^* from the single-particle spectrum dominates, so oscillation frequency decreases with Ω. When $\eta > \eta_0$, the effective mass m_I^* from interaction dominates, so oscillation frequency increases with Ω. Unlike the uniform case, η_0 is not a constant in the trap, but decreases with the chemical potential. The lowest collective mode is a combination of dipole mode and breathing mode. The other collective modes that we have not studied in this paper should be also combinations of modes with odd and even parity to satisfy Eqs. (31)–(34). The collective modes of a SO-coupled BEC in the plane-wave phase have no certain parity. Because the plane-wave phase spontaneously breaks the space-inversion symmetry. In the regime $\Omega > k_0^2/m$, there are SO coupling and broken invariance of SU(2) spin rotation, and the dipole mode and breathing mode are decoupled. This is the restriction of symmetry since in the $\Omega > k_0^2/m$ regime the ground state maintains the space-inversion symmetry and the coupling between the dipole mode and breathing mode is forbidden. Therefore, the SO coupling and broken invariance of SU(2) spin rotation are not the sufficient conditions for coupling of dipole mode and breathing mode. One needs to consider the symmetry restriction.

For the general situation with $h \neq 0$ and $g_{11} \neq g_{22}$, the Hamiltonian is not invariant under space inversion, so there is not symmetry restriction. The physical properties of the collective modes in the plane-wave phase will not change qualitatively. If $h \neq 0$, the single-particle spectrum still has the double-well structure in the small Ω regime. However, the depths of the two wells are not symmetric. The SU(2) spin rotation symmetry is also broken for $g_{11} \neq g_{22}$. So the competition between the effective mass and the interaction energy still plays an important role in the collective modes. The only difference is that the effective mass m_S^* is determined by both Ω and h, and another parameter is needed to describe the asymmetry of the spin-dependent interaction. In the large Rabi coupling regime, since the Hamiltonian breaks the space-inversion symmetry, the dipole mode and the breathing mode could be coupled together just like the plane-wave phase.

ACKNOWLEDGMENTS

W.Z. thanks Hui Zhai for introducing him to the subject and helpful discussion. The project is supported by the NSFC under Grant No. 10874249.

[1] X. L. Qi and S. C. Zhang, Phys. Today **63**, 33 (2010); M. Z. Hasan and C. L. Kane, Rev. Mod. Phys. **82**, 3045 (2010); X. L. Qi and S. C. Zhang, *ibid.* **83**, 1057 (2011).

[2] J. Dalibard, F. Gerbier, G. Juzeliūnas, and P. Öhberg, Rev. Mod. Phys. **83**, 1523 (2011).

[3] Y.-J. Lin, R. L. Compton, A. R. Perry, W. D. Phillips, J. V. Porto, and I. B. Spielman, Phys. Rev. Lett. **102**, 130401 (2009).

[4] Y.-J. Lin, R. L. Compton, K. Jiménez-García, J. V. Porto, and I. B. Spielman, Nature (London) **462**, 628 (2009).

[5] Y.-J. Lin, R. L. Compton, K. Jiménez-García, W. D. Phillips, J. V. Porto, and I. B. Spielman, Nat. Phys. (London) **7**, 531 (2011).

[6] Y.-J. Lin, K. Jiménez-García, and I. B. Spielman, Nature (London) **471**, 83 (2011).

[7] T. D. Stanescu, B. Anderson, and V. Galitski, Phys. Rev. A **78**, 023616 (2008); C. Wu and I. Mondragon-Shem, Chin. Phys. Lett. **28**, 097102 (2011); M. Merkl, A. Jacob, F. E. Zimmer, P. Öhberg, and L. Santos, Phys. Rev. Lett. **104**, 073603 (2010); H. Hu, B. Ramachandhran, H. Pu, and X. Liu, *ibid.* **108**, 010402 (2012); S. K. Yip, Phys. Rev. A **83**, 043616 (2011); Z. F. Xu, R. Lü, and L. You, *ibid.* **83**, 053602 (2011); S. Gopalakrishnan, A. Lamacraft, and P. M. Goldbart, *ibid.* **84**, 061604(R) (2011); T. Ozawa and G. Baym, *ibid.* **85**, 013612 (2012).

[8] T. L. Ho and S. Zhang, Phys. Rev. Lett. **107**, 150403 (2011).

[9] Chunji Wang, Chao Gao, Chao-Ming Jian, and Hui Zhai, Phys. Rev. Lett. **105**, 160403 (2010).

[10] T. Ozawa and G. Baym, Phys. Rev. A **84**, 043622 (2011); Qizhong Zhu, Chuanwei Zhang, and Biao Wu, e-print arXiv:1109.5811; R. Barnett *et al*., Phys. Rev. A **85**, 043622 (2012); K. Zhou and Z. Zhang, Phys. Rev. Lett. **108**, 025301 (2012).

[11] Chao-Ming Jian and Hui Zhai, Phys. Rev. B **84**, 060508(R) (2011).

[12] X. Q. Xu and J. H. Han, Phys. Rev. Lett. **107**, 200401 (2011); X.-Fa Zhou, J. Zhou, and C. Wu, Phys. Rev. A **84**, 063624 (2011); J. Radić, T. A. Sedrakyan, I. B. Spielman, and V. Galitski, *ibid.* **84**, 063604 (2011); Y. Deng, J. Cheng, H. Jing, C.-P. Sun, and S. Yi, Phys. Rev. Lett. **108**, 125301 (2012); T. Graß, K. Saha, K. Sengupta, and M. Lewenstein, Phys. Rev. A **84**, 053632 (2011).

[13] P. Wang, Z. Yu, Z. Fu, J. Miao, L. Huang, S. Chai, H. Zhai, and J. Zhang, e-print arXiv:1204.1887.

[14] D. S. Jin, J. R. Ensher, M. R. Matthews, C. E. Wieman, and E. A. Cornell, Phys. Rev. Lett. **77**, 420 (1996).

[15] M.-O. Mewes, M. R. Andrews, N. J. van Druten, D. M. Kurn, D. S. Durfee, C. G. Townsend, and W. Ketterle, Phys. Rev. Lett. **77**, 988 (1996).

[16] L. Pitaevskii and S. Stringari, *Bose-Einstein Condensation* (Oxford, New York, 2003).

[17] F. Zambelli and S. Stringari, Phys. Rev. Lett. **81**, 1754 (1998); F. Chevy, K. W. Madison, and J. Dalibard, *ibid*. **85**, 2223 (2000).

[18] D. Guéry-Odelin and S. Stringari, Phys. Rev. Lett. **83**, 4452 (1999); O. M. Marago, S. A. Hopkins, J. Arlt, E. Hodby, G. Hechenblaikner, and C. J. Foot, *ibid*. **84**, 2056 (2000).

[19] A. Polkovnikov and D. W. Wang, Phys. Rev. Lett. **93**, 070401 (2004); C. D. Fertig, K. M. O'Hara, J. H. Huckans, S. L. Rolston, W. D. Phillips, and J. V. Porto, *ibid*. **94**, 120403 (2005).

[20] L. Pitaevskii and S. Stringari, Phys. Rev. Lett. **81**, 4541 (1998); A. Altmeyer, S. Riedl, C. Kohstall, M. J. Wright, R. Geursen, M. Bartenstein, C. Chin, J. H. Denschlag, and R. Grimm, *ibid.* **98**, 040401 (2007).

[21] Y. Zhang, L. Mao, and C. Zhang, Phys. Rev. Lett. **108**, 035302 (2012).

[22] S. Chen, J. Zhang, S. Ji, Z. Chen, L. Zhang, Z. Du, Y. Deng, H. Zhai, and J. Pan, e-print arXiv:1201.6018.

[23] L. J. LeBlane *et al*., e-print arXiv:1201.5857.

[24] C. J. Pethick and H. Smith, *Bose-Einstein Condensation in Dilute Gases* (Cambridge, New York, 2002).

[25] R. Dum and M. Olshanii, Phys. Rev. Lett. **76**, 1788 (1996).

[26] G. Juzeliūnas and P. Öhberg, Phys. Rev. Lett. **93**, 033602 (2004).

[27] M. R. Andrews, D. M. Kurn, H.-J. Miesner, D. S. Durfee, C. G. Townsend, S. Inouye, and W. Ketterle, Phys. Rev. Lett. **79**, 553 (1997).

[28] J. Steinhauer, R. Ozeri, N. Katz, and N. Davidson, Phys. Rev. Lett. **88**, 120407 (2002).